Hybrid State Space Modelling of an SI Engine for Online Fault Diagnosis

Nadeer E P[1], Amit Patra[2], and Siddhartha Mukhopadhyay[3]

[1,2,3] *Indian Institute of Technology, Kharagpur, West Bengal, 721302, India*

epnadeer@iitkgp.ac.in

amit@ee.iitkgp.ernet.in

smukh@ee.iitkgp.ernet.in

Abstract

In this work, a nonlinear hybrid state space model of a complete spark ignition (SI) gasoline engine system from throttle to muffler is developed using the mass and energy balance equations. It provides within-cycle dynamics of all the engine variables such as temperature, pressure and mass of individual gas species in the intake manifold, cylinder and exhaust manifold. The inputs to the model are same as that are commonly exercised by the Engine Control Unit (ECU) and its outputs correspond to available engine sensors. It uses generally known engine parameters, does not require extensive engine maps found in mean value models and requires minimal experimentation for tuning. It is demonstrated that the model is able to capture a variety of engine faults by suitable parameterization. The state space modelling is parsimonious in having the minimum number of integrators in the model by appropriate choice of state. It leads to great computational efficiency due to the possibility of deriving the Jacobian expressions analytically in applications such as on-board state estimation. The model was validated both with data from an industry standard engine simulator and those from an actual engine after relevant modifications. For the test engine, the engine speed and crank-angle were extracted from the crank position sensor signal. The model was seen to match the true values of engine variables both in simulation and experiments.

1. Introduction

Automotive engine models based on physical first principles can be classified based on their modelling schemes and application domains. Based on the modelling schemes, they could be classified into Computational Fluid Dynamics (CFD) models, Mean Value Models

(MVMs), Discrete Event Models (DEMs) and Hybrid Models (HMs). Based on the application domain, the models may be classified into Design and Analysis Models, Control Oriented Models (COMs) and Diagnosis Oriented Models (DOMs). Note that models could overlap in many cases. Hybrid Models incorporate both continuous and discrete dynamics. The MVMs are a subset of continuous models and DEMs are of discrete nature. For control purposes, some subsystems are modelled as MVMs and some as DEMs, giving rise to HMs. For diagnosis purposes too, both MVMs and DEMs have been used. A brief literature map of engine models is given in Table 1.

Table 1: Literature map on engine modelling

Purpose	Model	Remarks
Engine design and analysis	CFD(e.g., [1], [2], [3])	Offline, One dimensional multi-zone models, Multidimensional models, Chemical kinetics
Engine controls	MVM [4][5][6] [7], HM (includes DEM) [8] [9]	MVMs: Maps and parameterization, Delay approximations, Cylinder assumed as a pump. DEMs: Discrete time models, Uses maps, delay approximations, constant speed assumptions (in some).
Engine diagnosis	MVM [10] [11], DEM [12], HM [13]	MVMs: Separate residual generators for individual subsystems, Fault isolability and identifiability issues. DEMs: Separate residual generators for individual subsystems. HMs: Long computation times and high sampling rates for full system model.

CFD models, such as the KIVA code [3] which employs three dimensional, multiphase, multi-component models, are indispensable in engine design and analysis, but require high computational capacity. The latest KIVA-4 could solve the dynamics on multiple distributed computers. However, the CFD models are yet to make it to online diagnosis schemes. With additional sensors on the engine system and powerful distributed off-board processors, they could be employed in future to provide both spatial and temporal information about faults.

Traditionally, MVMs have been used for both control and diagnosis purposes. MVMs for an SI engine with EGR were developed in [4] and [5]. In [6] and [7], Eriksson et al. adopt a component-wise mean value modelling strategy, with interactions between components defined based on physics and thermodynamics. Notably, the air flow into the cylinders is modelled using volumetric efficiency, which is either mapped or parameterized. This limits access to in-cylinder variables which can be crucial for diagnosis of cylinder faults. On the diagnosis side, pioneering works of Nyberg et al. (e.g., [10] and [11]) also use MVMs for detection and isolation of faults, adopting the component-wise strategy. Separate MVMs for fault diagnosis of individual components like air intake system [14], fuel system [15], and exhaust system [16] are also common in literature. However, MVMs fail to detect and/or isolate many of the faults occurring in the engine system. Identification of faults is even more difficult. They also require parameter maps developed by extensive experiments for model accuracy.

As for DEMs, in [8] and [9], Balluchi et al. have employed them for modelling the cylinders in the engine system. MVMs were employed for powertrain and intake manifold dynamics, making the overall model an HM. However, the purpose being controller design, the cylinder pressures and torques generated by individual cylinders were the engine variables used in the formulation, and the DEM for cylinder does not provide detailed within-cycle values of other cylinder variables. A detailed cylinder dynamical model for fault diagnosis purpose, developed in [17], using cylinder pressure and combustion heat release as the output variables and engine speed as an input, does not consider the engine system in totality. The cylinder-by-cylinder engine model (CCEM) discussed in [18] is also an example of DEM. A hybrid model of engine for misfire detection has been proposed in [12] in which the power generated during combustion is considered as an input and the engine speed as the output. More recently, a crank angle model for diesel engine was developed in [19] for hardware in loop (HIL) simulations.

A hybrid one-dimensional model of the entire engine system was developed in [13] for fault diagnosis, and was referred to as a Within Cycle Crank-angle based Model (WCCM). The WCCM considers pressures and temperatures at the intake manifold (IM), exhaust manifold (EM), and cylinder as state variables. The WCCM could be considered as an HM, where the state transitions occur in accordance with the switching conditions corresponding to flow rate reversals and engine strokes. However, the choice of state in [13] does not let the engine equations to be written in the state space form, and additional integrations of masses

of different gas species in IM, cylinder and EM were carried out, leading to redundancy in equations and long execution times. Further, the implementation of WCCM was offline and was validated only by simulation.

Due to the ability to capture within cycle details, as demonstrated in [13], the WCCM is capable of better fault detection and isolation as compared with MVM, albeit with greater computational effort. WCCM development requires less experimentation as most of the parameters are related to engine geometry and are readily available. **Figure 1** shows an online fault diagnosis scheme in which WCCM could be employed. It could be used inside nonlinear estimators/observers for accurate estimation of engine variables that are usually not measured, such as the pressures, temperatures and masses of individual gas species in cylinders. These variables contain fault signatures needed for fault detection and isolation. Being a diagnosis-oriented model, the WCCM has the advantage of accessing control signals coming out of ECU, and can improve the diagnosis functionality. Further, such a model when implemented online could help the ECU in implementing fault tolerant control schemes and integrated vehicle health management (IVHM). Note that even for fault tolerant control, unlike control-oriented models, diagnosis models need not have to be hard real time, allowing for more complexity to be added to the model for better diagnosability.

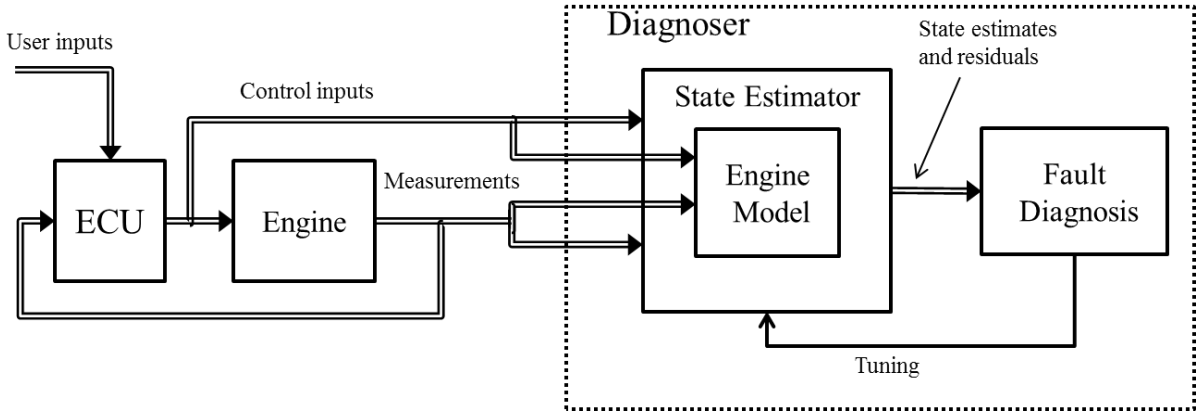

Figure 1: Fault diagnosis scheme using a within-cycle model

In this work, a minimal hybrid state space model of an *N*-cylinder engine system with Exhaust Gas Recirculation (EGR), from throttle to muffler, to be used for online estimation and fault diagnosis purposes is developed by reformulating the mass and energy balance equations. The modelling assumptions here are the same as that in [13], but the number of integrators needed for solving the state equation is less. The state variables are temperatures and masses of individual gas species at IM, EM and cylinder. The pressures are obtained by

an algebraic relation from the state variables. The model was implemented in Simulink™ for ease of conversion to executable code on ECU for online fault diagnosis. With the consistent choice of state variable at each reservoir, it is possible to have a reusable routine for evaluating Jacobian matrix of the system analytically at each reservoir, and can be used in online estimators such as the Extended Kalman Filter (EKF). The model is validated with an AMESim™ simulation of the engine. The model was also validated with data from an actual two-cylinder engine with no EGR, after relevant modifications. The model takes throttle position, fuel injector signals, EGR control signal, engine speed and crank-angle signals as inputs. The engine speed and crank-angle can be extracted from the crank position sensor signal. The measurements which are not designated as model inputs can be fed to the state estimator as the measurement vector. To capture various faults, suitable parameterization if the model is proposed, and the simulations indicate how the model produces adequate fault signatures for detection and isolation of faults.

2. State Space Modelling of an SI Engine

A naturally aspirated spark ignition (SI) gasoline engine has the basic subsystems and components shown in **Figure 2**, which include the intake manifold, combustion chamber (cylinder and piston), exhaust manifold, crank assembly, EGR, ECU, fuel injection and sensor and actuator assembly. A physical system such as engine consists of two kinds of objects: reservoirs and flows. Reservoirs store thermal or kinetic energy, mass, information, etc., whereas flows have these storage entities flowing between reservoirs, typically driven by differences in reservoir levels [20]. In the case of engine, we consider the intake manifold (IM), cylinder and exhaust manifold (EM) as reservoirs. The throttle, exhaust gas recirculation (EGR) and muffler are considered as flow elements. In **Figure 2**, the solid rectangles indicate flow elements, rounded rectangles the reservoirs, and dashed rectangle the other engine system components including ECU–which are not modelled. The engine intake and exhaust valves, which are considered as flow elements, are not shown in the Figure. The equations we employ here are from standard models available in duly mentioned references, the novelty is only in the state space formulation.

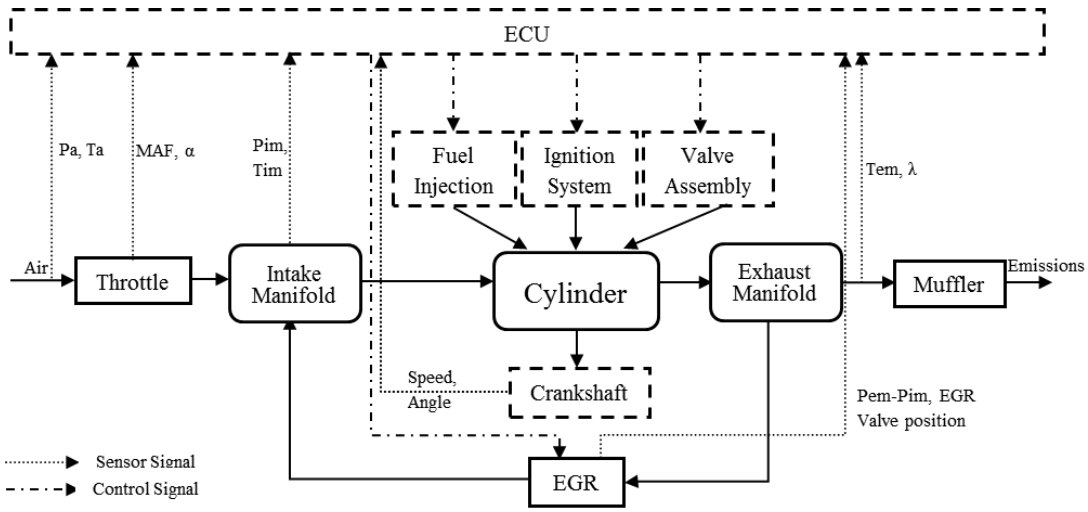

Figure 2: Block diagram of the SI engine system

A full 4-stroke engine cycle corresponds to a crank shaft rotation of 0-720°, approximately 180° each for intake, compression, expansion and exhaust strokes. Detailed working of engine and thermodynamic models of individual components are available in standard textbooks, see for e.g., [21]. The WCCM equations essentially describe two things: the continuous time dynamics (or flows) of the variables or system states of interest – such as pressure, temperature and mass flow rates – and the jump conditions, or events, which cause transition between different modes of the hybrid system. These transitions between modes could be triggered either by control actions, or by the instantaneous state variable values themselves (e.g., sub-sonic or sonic, positive flow or negative flow), or by the different strokes of the engine. These transitions are embedded by using signum functions in the first order differential equations we are about to derive.

A summary of main engine variable notations and subscripts used is given in Table 2. Each variable on the left column appears with one or more of the subscripts from the right column in the model equations.

We assume that all the gases in the engine obey the ideal gas law, i.e.

$$PV = mRT \qquad \textbf{(1)}$$

Note that all variables are functions of time t, although we have omitted it for convenience. All variables are in their SI units. The R in above expression is the specific gas constant, not universal gas constant, and mass m is in kg.

Table 2: Variable and subscript notations

Variables		Subscripts	
P	Pressure	in	Variable in to control volume/flow element
V	Volume	out	Variable out of control volume/flow element
m	Mass	th	Throttle
R	Specific gas constant	im	Intake manifold
T	Temperature	cyl	Cylinder
$\dot{m}$	Mass flow rate	em	Exhaust manifold
C_p	Specific heat at constant pressure	egr	Exhaust gas recirculation
C_v	Specific heat at constant volume	muf	Muffler
γ	Ratio of specific heats	i2c	Intake manifold to cylinder
ω	Engine speed	c2e	Cylinder to exhaust manifold
θ	Crank angle	a	Air
H	Enthalpy	b	Burnt gases
U	Internal energy	f	Fuel
Q	Heat energy	cool	Cooling (temperature)
W	Work	amb	Ambient

Ignoring the changes in kinetic and potential energy in the flow, the transient mass and energy balance equations describing the reservoir can be written in terms of the rates of mass *m*, the enthalpy *H*, the internal energy *U*, the heat energy added to the system *Q*, and shaft work done on the system *W*, as [22] :

$$\begin{aligned} \dot{m} &= \sum_i \dot{m}_{i,in} - \sum_i \dot{m}_{i,out} \\ \dot{U} &= \dot{H}_{\text{in}} - \dot{H}_{\text{out}} + \dot{Q} + \dot{W} \end{aligned} \tag{2}$$

where the subscripts *in* and *out* capture not only the input and output variables, but also the generated and consumed variables, respectively, at the reservoir. The index *i* stands for different gas species.

The flow equation for the valves can be written as [20]:

$$\dot{m} = C_d A \frac{P_{\text{in}}}{\sqrt{R_{\text{in}} T_{\text{in}}}} \psi \left(\frac{P_{\text{in}}}{P_{\text{out}}} \right) \tag{3}$$

where,

$$\psi\left(\frac{P_{\text{in}}}{P_{\text{out}}}\right)=\begin{cases}\sqrt{\gamma_{\text{in}}\left[\frac{2}{\gamma_{\text{in}}+1}\right]^{\frac{\gamma_{\text{in}}+1}{\gamma_{\text{in}}-1}}}, & P_{\text{out}}<P_{\text{cr}}\\ \left(\frac{P_{\text{out}}}{P_{\text{in}}}\right)^{\frac{1}{\gamma_{\text{in}}}}\sqrt{\frac{2\gamma_{\text{in}}}{\gamma_{\text{in}}-1}\left[1-\left(\frac{P_{\text{out}}}{P_{\text{in}}}\right)^{\frac{\gamma_{\text{in}}-1}{\gamma_{\text{in}}}}\right]}, & P_{\text{out}}\geq P_{\text{cr}}\end{cases} \quad \textbf{(4)}$$

and,

$$P_{cr}=2/(\gamma_{in}+1)^{\frac{\gamma_{in}}{\gamma_{in}-1}}P_{in} \quad \textbf{(5)}$$

Note that in the above expression the subscripts *in* and *out* have been used assuming a forward flow, with P_{in} being upstream and P_{out} downstream. They will be interchanged for reverse flow with a negative sign attached to the equation. Also, γ_{in} value is the ratio of specific heats for the upstream gas species.

At each reservoir, the specific gas constant and specific heats can be expressed as:

$$R=\frac{\sum m_i R_i}{m},\ C_p=\frac{\sum m_i C_{p,i}}{m},\ C_v=\frac{\sum m_i C_{v,i}}{m},\ \gamma=C_p/C_v \quad \textbf{(6)}$$

where, i=*a,b,f* (for air, burnt gases and fuel), and $m=m_a+m_b+m_f$ **(7)**

The time derivative of internal energy can be expressed in terms of masses, specific heats and temperature at the reservoir as:

$$\begin{aligned}\dot{U}&=mC_v\dot{T}+m\dot{C}_vT+\dot{m}C_vT=mC_v\dot{T}+\left(m\dot{C}_v+\dot{m}C_v\right)T\\&=mC_v\dot{T}+\left(\sum_i\dot{m}_iC_{v,i}\right)T\end{aligned} \quad \textbf{(8)}$$

The net flow rate of enthalpy into a reservoir can be expressed in terms of the flow rates of individual species of air, burnt gases, and fuel entering and leaving the reservoirs.

$$\Delta\dot{H}=\dot{H}_{\text{in}}-\dot{H}_{\text{out}}=\sum_i\dot{m}_{\text{i,in}}C_{p_{\text{i,in}}}T_{\text{in}}-\sum_i\dot{m}_{\text{i,out}}C_{p_{\text{i,out}}}T_{\text{out}} \quad \textbf{(9)}$$

We choose a minimal state vector as:

$$x=\left[m_{\text{im,i}},T_{\text{im}},m_{\text{cyl,i}},T_{\text{cyl}},m_{\text{em,i}},T_{\text{em}}\right]^T \quad \textbf{(10)}$$

where, i = *a,b,f* (air, burnt gases, fuel). m_{cyl} and T_{cyl} are vectors with elements denoting the mass and temperature for individual cylinders. It will be shown that by this choice of state, it

is possible to express the nonlinear engine dynamical equations in the form $\dot{x} = f(x,u,t)$ where u is the input vector.

The state space formulation requires that all the variables be expressed in terms of inputs, states and their first order derivatives. The pressure P and specific heats C_p and C_v at a reservoir can be expressed in terms of other states using the assumptions in Eq. (6). The derivative of C_v in Eq. (8) was also expressed in terms of states and their derivatives by differentiating the expression for C_v in Eq. (6).

2.1. Model Inputs

The model inputs are: Throttle position, Fuel control signal, EGR control signal, speed and crank angle. For the experimental engine, since there is no EGR, the EGR control signal is not present. Note that in case we use the engine torque and speed model, the angular engine speed becomes a state rather than an input. Also, crank angle (θ) is simply the integral of speed, and hence that can also be considered a state, and can be computed if we know the initial angle.

The engine speed and crank-angle position signals, which our model assumes as inputs, are usually not available as direct measurements, and hence need to be extracted from other measurements. The crank-shaft position sensor, which could be of variable reluctance (VR) type or Hall-effect type, is usually present in all cars. Our experimental engine has a VR type sensor. The VR sensor output signal has a varying amplitude and frequency depending on the engine speed. The spikes in sensor signal correspond to missing teeth positions on the flywheel connected to the crankshaft. At low engine speeds, a sampling period of 1ms is sufficient for extracting the average engine speed and crank angle. However, at higher engine speeds, a sampling period of 0.1ms was found to be necessary to extract speed and crank-angle from the crank signal.

2.1.1. Extraction of speed and crank angle from crank position sensor signal

1. Detect the first instance of missing teeth from the crank pulses and initialize the crank angle to the value corresponding to missing teeth location on flywheel. Initialize pulse count to one. Initialize speed to an arbitrary value.
2. For each rising edge of the pulse add 10^0(=360/36) to the crank angle and increase the pulse count by one. For the time instants in between pulses, interpolate the crank angle using the speed data from the previous cycle. When

the pulse count reaches 35, add 20^0 to the crank angle and reset the pulse count back to one. Find the time elapsed since the last cycle ΔT (for 360^0 rotation) and obtain the speed in rad/s as $\omega = \frac{2\pi}{\Delta T}$. Pass this signal through a low pass filter to eliminate noise.

3. Reset the crank angle to zero when it reaches 720^0.

In a similar manner, in case of a sample rate constraint, the fuel injector signal available from the ECU could be used for engine speed and crank angle determination.

2.2. Intake and Exhaust Manifold Models:

The mass balance at IM is:

$$\dot{m}_{\text{im}} = \dot{m}_{\text{th}} + \dot{m}_{\text{egr}} - \dot{m}_{\text{i2c}} \tag{11}$$

Where m_{th} and m_{egr} stand for the mass flow rates at throttle and EGR respectively, and m_{i2c} is the flow rate of gas entering the cylinder from IM. These can be obtained at every time instant by using Eq. (3). Replacing the pressures P_{in} and P_{out} in Eq. (3) by Eq. (1), and the ratio of specific heats γ_{in} from Eq. (6), it can be seen that all the terms in Eq. (11) are expressed purely in terms of the states in Eq. (10). The individual mass flow rates m_i for air, burnt gases and fuel can be obtained from the above relation by multiplying each of these flow rates by the individual fractions from the previous time instant. Considering m_i as states, from Equations (1) and (6), it follows that, unlike the choice of state in [13] only one of P and T needs to be considered as a state variable, since the other could then be obtained by an algebraic relation.

The dynamics for temperature T at the IM can be obtained from enthalpy balance in Eq. (2), by ignoring the shaft work term. From the assumptions on C_p and C_v in Eq. (6) and the thermodynamic expressions for enthalpy and internal energy the energy balance gives:

$$\dot{T}_{\text{im}} = \frac{1}{m_{\text{im}} C_{v_{\text{im}}}} \begin{pmatrix} \dot{m}_{\text{th}} \left(\sigma_{\dot{m}_{\text{th}}} C_{p_a} T_a + (1-\sigma_{\dot{m}_{\text{th}}}) C_{p_{\text{im}}} T_{\text{im}} \right) \\ + \dot{m}_{\text{egr}} \left(\sigma_{\dot{m}_{\text{egr}}} C_{p_{\text{em}}} T_{\text{em}} + (1-\sigma_{\dot{m}_{\text{egr}}}) C_{\text{p}_{\text{im}}} T_{\text{im}} \right) \\ - \sum_{i=1}^{N} \left(\dot{m}_{\text{i2c,i}} \left(\sigma_{\dot{m}_{\text{i2c,i}}} C_{p_{\text{im}}} T_{\text{im}} + (1-\sigma_{\dot{m}_{\text{i2c,i}}}) C_{\text{p}_{\text{cyl,i}}} T_{\text{cyl,i}} \right) \right) \\ - h_{\text{c,im}} A_{\text{c,im}} \left(T_{\text{im}} - T_{\text{cool,im}} \right) - \left(\sum \dot{m}_{\text{im,i}} C_{\text{v}_{\text{im}},\text{i}} \right) T_{\text{im}} \end{pmatrix} \tag{12}$$

where, $\sigma_{\dot{m}} = \left(\frac{1+\text{sgn}[\dot{m}]}{2}\right)$, sgn(.) denoting the signum function and N is the number of cylinders . The heat energy lost due to convection is also included in the above equation with $h_{\text{c,im}}$ being the heat transfer coefficient and $A_{\text{c,im}}$ the effective area.

Mass and energy balance at the exhaust manifold gives similar expressions:

$$\dot{m}_{\text{em}} = \dot{m}_{c2e} - \dot{m}_{\text{egr}} - \dot{m}_{\text{muf}} \tag{13}$$

where m_{c2e} is the cylinder-to-exhaust flow rate and m_{muf} is the muffler flow rate.

$$\dot{T}_{\text{em}} = \frac{1}{m_{\text{em}} C_{\text{v}_{\text{em}}}} \begin{pmatrix} \sum_{i=1}^{N} \left(\dot{m}_{\text{c2e,i}} \left(\sigma_{\dot{m}_{\text{c2e,i}}} C_{\text{p}_{\text{cyl,i}}} T_{\text{cyl,i}} + (1-\sigma_{\dot{m}_{\text{c2e,i}}}) C_{p_{\text{em}}} T_{\text{em}} \right) \right) \\ -\dot{m}_{\text{muf}} \left(\sigma_{\dot{m}_{\text{muf}}} C_{p_{\text{em}}} T_{\text{em}} + (1-\sigma_{\dot{m}_{\text{muf}}}) C_{\text{p}_{\text{a}}} T_{\text{a}} \right) \\ -\dot{m}_{egr} \left(\sigma_{\dot{m}_{\text{egr}}} C_{p_{\text{em}}} T_{\text{em}} + (1-\sigma_{\dot{m}_{\text{egr}}}) C_{\text{p}_{\text{im}}} T_{\text{im}} \right) \\ -h_{\text{c,em}} A_{\text{c,em}} \left(T_{\text{em}} - T_{\text{cool,em}} \right) - \left(\sum \dot{m}_{\text{em,i}} C_{\text{v}_{\text{em}},\text{i}} \right) T_{\text{em}} \end{pmatrix} \tag{14}$$

2.3. Cylinder Model

The mass balance equation for individual cylinders could be written as

$$\dot{m}_{\text{cyl}} = \dot{m}_{\text{i2c}} - \dot{m}_{\text{c2e}} + \dot{m}_f, \tag{15}$$

where m_f is the fuel input flow rate. During combustion, the total mass flow rate is zero, but the air and fuel get converted to burnt gases, changing individual component rates. These rates can be calculated for the i^{th} cylinder as,

$$\begin{aligned} \dot{m}^{(i)}_{\text{cyl,a}} &= \dot{m}^{(i)}_{\text{i2c}} \left(\sigma_{\dot{m}^{(i)}_{\text{i2c}}} \frac{m_{\text{im,a}}}{m_{\text{im}}} + (1-\sigma_{\dot{m}^{(i)}_{\text{i2c}}}) \frac{m^{(i)}{}_{\text{cyl,a}}}{m^{(i)}{}_{\text{cyl}}} \right) \\ &\quad - \dot{m}^{(i)}_{\text{c2e}} \left(\sigma_{\dot{m}^{(i)}_{\text{c2e}}} \frac{m^{(i)}{}_{\text{cyl,a}}}{m^{(i)}{}_{\text{cyl}}} + (1-\sigma_{\dot{m}^{(i)}_{\text{c2e}}}) \frac{m_{\text{em,a}}}{m_{\text{em}}} \right) - \frac{m^{(i)}_{\text{fb}} \lambda_{\text{af}} \omega}{\Delta\theta} \\ \dot{m}^{(i)}_{\text{cyl,f}} &= \dot{m}^{(i)}_{\text{i2c}} \left(\sigma_{\dot{m}^{(i)}_{\text{i2c}}} \frac{m_{\text{im,f}}}{m_{\text{im}}} + (1-\sigma_{\dot{m}^{(i)}_{\text{i2c}}}) \frac{m^{(i)}{}_{\text{cyl,f}}}{m^{(i)}{}_{\text{cyl}}} \right) \\ &\quad - \dot{m}^{(i)}_{\text{c2e}} \left(\sigma_{\dot{m}^{(i)}_{\text{c2e}}} \frac{m^{(i)}{}_{\text{cyl,f}}}{m^{(i)}{}_{\text{cyl}}} + (1-\sigma_{\dot{m}^{(i)}_{\text{c2e}}}) \frac{m_{\text{em,f}}}{m_{\text{em}}} \right) - \frac{m^{(i)}_{\text{fb}} \omega}{\Delta\theta} + \dot{m}^{(i)}_f \\ \dot{m}^{(i)}_{\text{cyl,b}} &= \dot{m}^{(i)}_{\text{cyl}} - \dot{m}^{(i)}_{\text{cyl,a}} - \dot{m}^{(i)}_{\text{cyl,f}} \end{aligned} \tag{16}$$

where $m_{\mathrm{fb}}^{(i)}$ is the mass of fuel accumulated in cylinder *i* before combustion, ω is the engine angular speed, λ_{af} is the stoichiometric air-fuel ratio and $\Delta\theta$ is the combustion duration angle. The fuel flow rate into the cylinder $\dot{m}_f^{(\mathrm{i})}$ could be calculated from the fuel injector signal coming out of ECU. The terms $\frac{m_{\mathrm{fb}}^{(i)}\lambda_{\mathrm{af}}\omega}{\Delta\theta}$ and $\frac{m_{\mathrm{fb}}^{(i)}\omega}{\Delta\theta}$ in the above expression appear only for the combustion duration.

In addition to the terms in enthalpy balance for IM and EM, the enthalpy balance for cylinder *i* should include the rate of heat energy added during combustion ($\dot{Q}_{\mathrm{comb}}$) – approximated by the Wiebe function [21]– and lost due to convection and radiation ($\dot{Q}_{\mathrm{heatloss}}$) [23], given by,

$$\begin{aligned}\dot{Q}_{\mathrm{comb}}^{(i)} &= \eta_{\mathrm{c}}^{(\mathrm{i})} m_{\mathrm{fb}}^{(i)} Q_{\mathrm{lhv}}\omega\frac{dx_b^{(i)}}{d\theta}\\ &= \frac{\eta_{\mathrm{c}}^{(\mathrm{i})} m_{\mathrm{fb}}^{(\mathrm{i})} Q_{\mathrm{lhv}}\omega na}{\Delta\theta}\left(\frac{\theta-\theta_{\mathrm{soc}}^{(\mathrm{i})}}{\Delta\theta}\right)^{n-1}\exp\left[-a\left(\frac{\theta-\theta_{\mathrm{soc}}^{(\mathrm{i})}}{\Delta\theta}\right)^{n}\right]\\ \dot{Q}_{\mathrm{heatloss}}^{(\mathrm{i})} &= h_c^{(\mathrm{i})}A_{\mathrm{c}}^{(\mathrm{i})}(T_{\mathrm{cyl}}^{(\mathrm{i})}-T_{\mathrm{cool}}^{(\mathrm{i})})+\varepsilon\sigma\left((T_{\mathrm{cyl}}^{(\mathrm{i})})^4-(T_{\mathrm{cool}}^{(\mathrm{i})})^4\right)\end{aligned} \quad \textbf{(17)}$$

where η_c is the combustion efficiency, Q_{lhv} the lower heating value of fuel, *a*, *n* the Wiebe parameters, x_b the burnt mass fraction, θ_{soc} the start of combustion angle, h_c the coefficient of convective heat transfer, A_c the effective area of convective heat transfer, ε is the emissivity of cylinder block material, and σ the Stefan-Boltzmann constant. At the cylinder, the enthalpy balance should also include the piston work, which for the i^{th} cylinder is given by $P_{cyl}^{(i)}\dot{V}_{cyl}^{(i)}$. Thus for the i^{th} cylinder, the expression for cylinder temperature derivative is

$$\dot{T}_{\mathrm{cyl}}^{(i)} = \frac{1}{m_{\mathrm{cyl}}^{(i)}Cv_{\mathrm{cyl}}^{(i)}}\begin{pmatrix}\dot{Q}_{\mathrm{comb}}^{(i)}-\dot{Q}_{\mathrm{heatloss}}^{(i)}+\dot{H}_{\mathrm{in}}^{(i)}-\dot{H}_{\mathrm{out}}^{(i)}\\ -T_{\mathrm{cyl}}^{(i)}\times\left(\sum\dot{m}_{\mathrm{cyl,j}}^{(i)}Cv_{\mathrm{cyl,j}}^{(i)}\right)-P_{\mathrm{cyl}}^{(i)}\dot{V}_{\mathrm{cyl}}^{(i)}\end{pmatrix}, \quad \textbf{(18)}$$

where the index *j* has been used for individual gas species. As before, all the terms on the RHS above should be expressed in terms of inputs and state. To express the time derivative of the cylinder volume $\dot{V}_{cyl}^{(i)}$ in terms of crank angle and speed input, we consider the expression for cylinder volume (index *i* dropped) [21],

$$V_{cyl} = \frac{V_d}{r_c - 1} + \frac{V_d}{2}\left(\frac{l}{r} + 1 - \cos\theta + \sqrt{\frac{l^2}{r^2} - \sin^2\theta} \right), \quad \textbf{(19)}$$

where V_d is the displacement volume, r_c is the compression ratio, l is the connecting rod length and r is the crank radius. Differentiating the above expression w.r.t time, we get

$$\dot{V}_{cyl} = \frac{dV_c}{d\theta}\frac{d\theta}{dt} = \frac{V_d}{2}\left(\sin\theta + \frac{\sin 2\theta}{2\sqrt{\frac{l^2}{r^2} - \sin^2\theta}} \right)\omega, \quad \textbf{(20)}$$

where ω is the angular speed.

Equations (11)– (18) constitute the first order non-linear differential equations necessary for forming the state space model, considering the speed ω and crank-angle θ as inputs. If, however, the speed and crank-angle are considered as states, and load torque as an input, an additional torque modelling is necessary.

2.4. Flow element models

The flow cross section area *A* in Eq. (3) depends on the flow element under consideration. In the engine system, the flow elements of interest to us are the throttle, the intake valve, the exhaust valve, the fuel inlet valve and the muffler. We consider the fuel flow rate as a constant, with the actual fuel input being controlled by pulse width modulation, and hence the orifice flow equation is not used for fuel flow.

2.4.1. The Throttle

For a manually controlled throttle, the flow cross section area is simply the open area of the butterfly valve, commonly used for letting the air in when the driver presses the gas pedal. During the vehicle idle condition in which the butterfly valve is closed, to keep the engine on, an idle air bypass valve is employed. This bypass valve is controlled by a stepper motor. The total area of the throttle considering both the valves is given by

$$A_{th} = \frac{\pi D_{th}^2}{4}\left(1 - \cos(\alpha_{th})\right) + A_{th,bypass}\ , \quad \textbf{(21)}$$

where D_{th} is the diameter of the butterfly valve, α_{th} is the butterfly valve angle, and $A_{th,bypass}$ is the effective area of the bypass valve. An accurate estimation of $A_{th,bypass}$ would require stepper motor and bypass valve modelling. Instead, we employ a crude correction by adding

an additional area to the butterfly valve area based on the stepper motor position (calculated in open loop from the stepper input signals available from the ECU) in order to match the intake manifold pressure.

2.4.2. Intake and Exhaust Valves

There are three flow elements associated with the cylinder: the intake valve, the exhaust valve and the fuel inlet valve. Intake and exhaust valve openings are usually controlled by an overhead camshaft, depending on the engine stroke. Effective flow cross-section area is the smallest area encountered by the flow, which changes depending on the valve lift. To calculate the valve open areas w.r.t the crank angle, a hundred data points for valve lift and crank angle were stored in a lookup table (LUT). By storing the valve lift instead of area, this LUT can be reused for engines having similar valve profiles, but different valve dimensions. The valve lift corresponding to any crank angle is then found by using the interpolation function in Matlab. For small valve lifts, the valve area is given by [24]

$$A_f(\theta) = \pi D_h L_v(\theta) \frac{1 + {D_p}/{D_h}}{2} \cos\theta_v \,, \tag{22}$$

where D_p is the valve port diameter, D_h is the valve head diameter, θ_v is the valve seat angle and L_v is the valve lift. The above expression is valid only up to a certain lift, after which the smallest area available for flow is the port area, given by [24]:

$$A_m = \pi D_p^2 / 4 \tag{23}$$

The minimum valve area is then found out for the lift value obtained from interpolation as:

$$A = \min\left(A_f, A_m\right) \tag{24}$$

2.4.3. The Muffler

We consider the muffler, which takes the exhaust gases out from the exhaust manifold as a flow element with the exhaust manifold pressure on one side and atmospheric pressure on other. The area of cross section is the effective area encountered by the gases exiting the exhaust manifold, and we assume this flow area to be a fixed value.

2.5. Solving the state equation

The continuous-time nonlinear engine dynamical equations need to be solved at every time step to obtain the state variables. The accuracy of the solutions depends on the integration method employed. An Euler discretization, while being easy to implement and fast in execution, is not very accurate for highly nonlinear systems like engine. Hence the Runge-Kutta 4^{th} order (RK4) method was employed for solving the equations in Simulink. Also, it was found that using this method, the non-Lipschitz nature of mass flow rate equation (during the situation when the upstream and downstream pressures are equal) does not affect the simulation time or accuracy significantly. The discretization sample time used for the model was 0.1ms. Note that this is only for the model execution, and the sensor sampling rates could be lower.

2.6. Model parameters and tuning

The parameters used in model development can be classified into three categories: general parameters, environmental parameters, and engine-specific parameters. General parameters include properties of gasoline, which was assumed to be the fuel for the developed model, such as the lower heating value, and properties of gases such as specific heats of air, burnt gases, and fuel. These could be assumed to be the same over all gasoline engines for which the model is to be used. Environmental parameters, which include the atmospheric temperature and pressure, may need to be changed according to the outdoor conditions either based on prior knowledge of environment or sensor measurements. Engine-specific parameters include all parameters related to engine geometry, fuel injection timings, valve lifts, valve timings and additional engine specific parameters such as the bypass valve area.

The engine specific parameters could either be plugged in by the user depending on the particular vehicle model and type, or be chosen from a list of parameter sets available for an array of engines. If some of the engine parameters are not known beforehand, they could either be found by experimentation, or could be learnt by online estimation during the model initialization phase assuming a non-faulty engine. Minor deviations in parameter values are acceptable provided they do not manifest as faults, since the estimator in which the model would be used could correct these deviations. The three types of parameters used in the model are listed in Table 3.

Note that in the model, the specific heats of air, burnt gases and fuel have been assumed to be constants. The values used were at the average temperatures for each reservoir. This could cause a minor accuracy issue for cylinder variables. If more accuracy is needed, the Janaf-Yaws expressions could be used to evaluate these values at each instant based on the cylinder temperature obtained from the model. This does not increase the number of state variables because the Janaf-Yaws values are entirely dependent on temperature. But the incorporation of the regression tables into the model increases memory requirement. Further, the slight increase in model accuracy does not improve fault diagnosability significantly.

Discharge coefficients in the range of 0.6–0.8 have been used for flow elements. Since these coefficients are clubbed with area, the differences would manifest as errors in areas. Tuning of these variables could be done so as to match the pressure variables under nominal operation.

The model was not found to be sensitive to coefficients of convective and radiative heat transfer, because most of the heat energy is exchanged through mass transfer. The combustion efficiency was taken to be 1, and values near 1, such as 0.98, do not affect the model variables significantly.

Table 3: Parameters used in the model

General parameters:	
$C_{p_a}, C_{p_b}, C_{p_f}, C_{v_a}, C_{v_b}, C_{v_f}$	Specific heats of air, burnt gases and fuel at average temperature
λ_{af}	Stoichiometric air fuel ratio
Q_{lhv}	Lower heating value of fuel
n, a	Wiebe function parameters
Environmental parameters:	
P_{amb}	Ambient pressure
T_{amb}	Ambient temperature
T_{fuel}	Fuel temperature
Engine-specific parameters:	
$C_{d,th}, C_{d,i}, C_{d,e}, C_{d,muf}, C_{d,egr}$	Discharge coefficient for flow elements (throttle, intake valve, exhaust valve, muffler and EGR valve)
D_{th}	Throttle butterfly valve diameter

$A_{th,bypass}$	Bypass valve area
D_p, D_h	Diameters of valve port and valve head
L_v	Valve lift
θ_v	Valve seat angle
θ_{soc}	Start of combustion angle
θ_{eoc}	End of combustion angle
$\Delta\theta$	Combustion duration angle (in *rad*)
η_c	Combustion efficiency
V_d	Cylinder displacement volume
r_c	Compression ratio
l	Connecting rod length
r	Crank shaft radius
h_c	Coefficient of convective heat transfer
A_c	Effective area of convective heat transfer

3. Fault Modelling

The sensor measurements from an actual engine could be compared with the signals generated by the engine model. If the model is accurate, any discrepancy between sensor measurements and model outputs could be due to faults. The model could be used inside a state estimator for better fault detection, using the residual signals – difference between actual and estimated measurements – for fault detection and isolation. It should be noted that modelling assumptions and choice of model parameters make some of the faults un-isolable.

To extend the fault detection, isolation and identification (FDD) capabilities, additional fault modelling could be used, thereby increasing the effective number of parameters in the model. The fault parameters should be able to capture a wide range of faults that could happen in the engine system. A good fault diagnosis model should be more sensitive to changes in fault parameters and less sensitive to modelling errors. However, these requirements are usually contradictory since the faults are themselves captured by changes in model parameters. Table 4 shows how some of the engine faults could be captured in the present modelling scheme.

The intake and exhaust manifold leaks could be modelled by additional areas in respective flow elements. The valve faults in cylinder could also be modelled the same way. Note that the valve faults could also manifest as misfire. For the case of manifold fuel injection, the misfire and fuel injector faults could be modelled separately, since the former affects only a particular cylinder while the latter affects all.

Table 4: Fault modelling for various faults in the engine system

	Faults	Modelling
Process and actuator faults	Intake manifold leak	Additional unknown area in the throttle
	Exhaust manifold leak	Additional unknown area in the muffler
	Misfire, Fuel injector fault	Multiplicative factor on fuel injection rate to individual cylinders
	Intake valve faults	Multiplicative/additive factor on intake valve area
	Exhaust valve faults	Multiplicative/additive factor on exhaust valve area
Sensor faults	Mass Air Flow (MAF) sensor bias	Additive term in measurement equation
	MAF sensor calibration fault	Multiplicative term in measurement equation
	Manifold Pressure and Temperature (TMAP) sensor bias	Additive term in measurement equation
	TMAP sensor calibration fault	Multiplicative term in measurement equation
	Exhaust pressure sensor bias	Additive term in measurement equation
	Exhaust pressure sensor calibration fault	Multiplicative term in measurement equation

4. Model simulation results

The instantaneous engine model described previously was implemented in Simulink^{TM}. This is convenient for conversion to hex code that could run on the ECU because all the tools required for such conversion already exist. Simulink model results were compared against an AMESim model of the engine. Model performance was evaluated using the Normalized Root Mean Square Error (NRMSE) for states, given by:

$$NRMSE = \sqrt{\frac{\sum_{i=1}^{n_s}\sum_{j=1}^{n_t}\left(\frac{x(i,j)-x_t(i,j)}{\max(x_t(i))\text{-}\min(x_t(i))}\right)^2}{n_s n_t}} \quad \textbf{(25)}$$

where $x(i,j)$ represents the i^{th} element of the state vector at j^{th} sampling instant from the developed model and $x_t(i,j)$ represents the same from AMESim model. n_s is the no. of state variables and n_t the no. of samples.

The throttle input applied was piecewise linear with 20^0 angle from 0-1.5s, linearly increasing from 20^0–70^0 during 1.5–2.5s, and remaining at 70^0 from 2.5–4s. The NRMSE value for all the states combined was 0.0433. Figure 3 shows the model state variables from Simulink compared with true state variables from AMESim for the full range of input. It could be seen that maximum deviation from the true model happens during the fast input transition. Detailed views of some variables are shown in Figure 4.

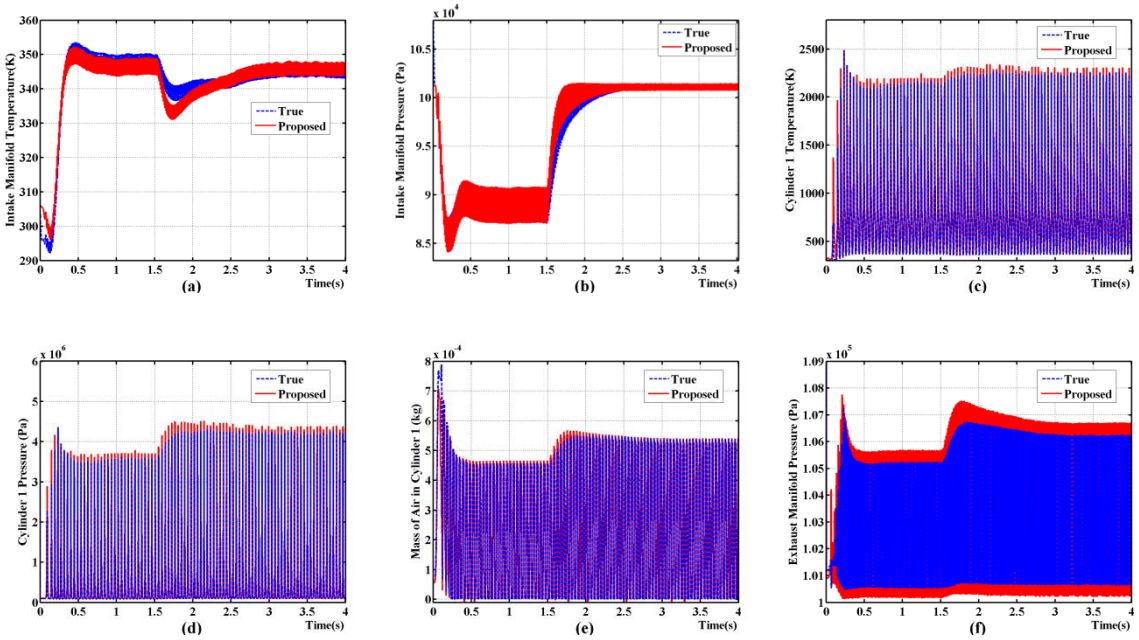

Figure 3: Engine variable plots for proposed and true models for the entire throttle range

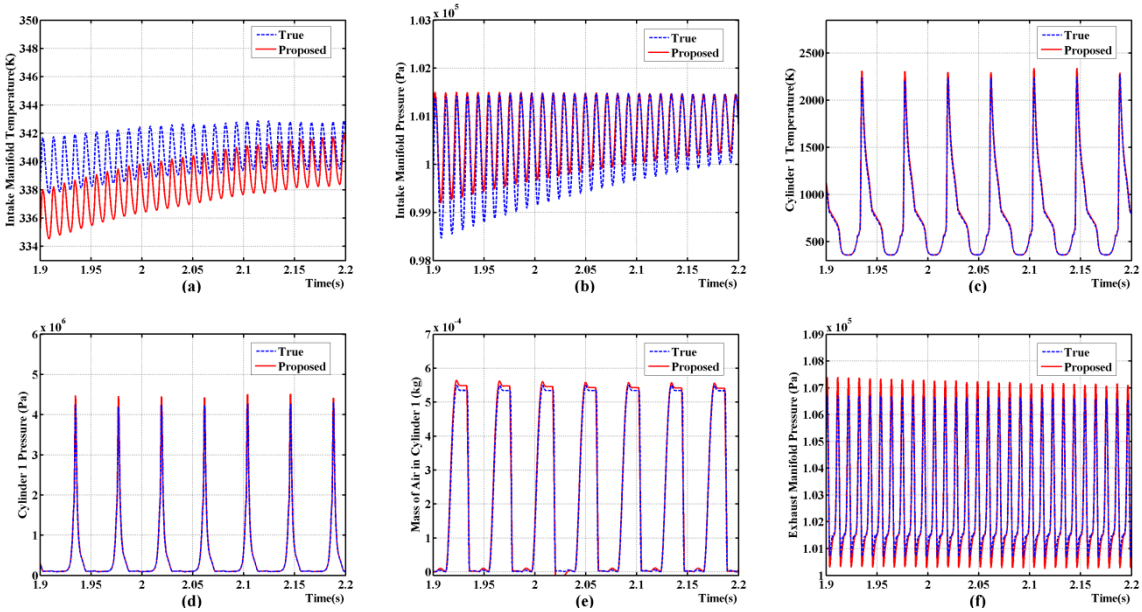

Figure 4: Detailed view of some engine variables from the proposed and true models

5. Fault simulation results

In this section we present the results of model simulation in presence of some of the faults listed in Table 4, namely the leak faults in intake manifold, exhaust manifold and cylinder; and injector fault in cylinder.

Figure 5 shows some of the engine variables under an IM leak fault of 50mm^2. The leak mainly affects the IM variables – air mass, pressure and temperature – only. Under an EM leak of area that is 10 percent of the muffler area, the IM variables are seen to be affected as well as EM variables (decreased pressure due to leak) , as shown in Figure 6. This is because of the EGR flow being reduced by the EM leak, lowering the IM temperature.

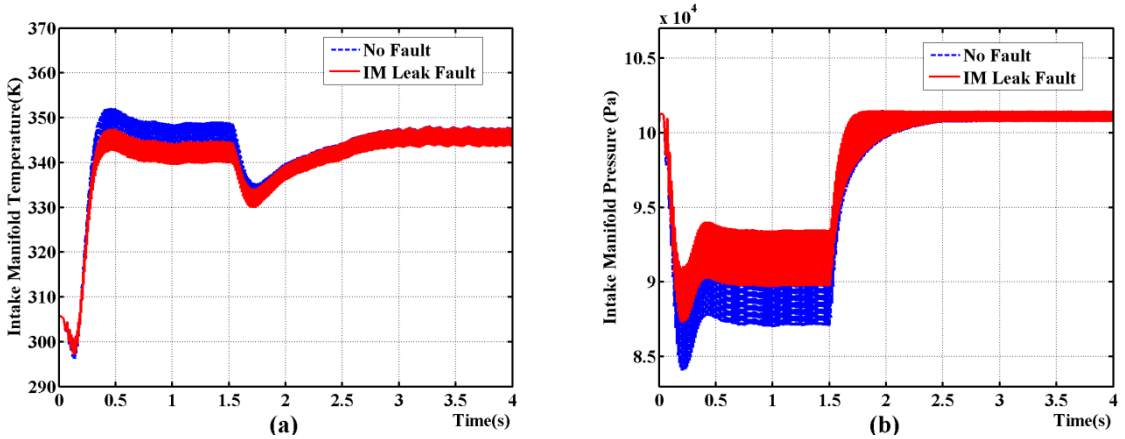

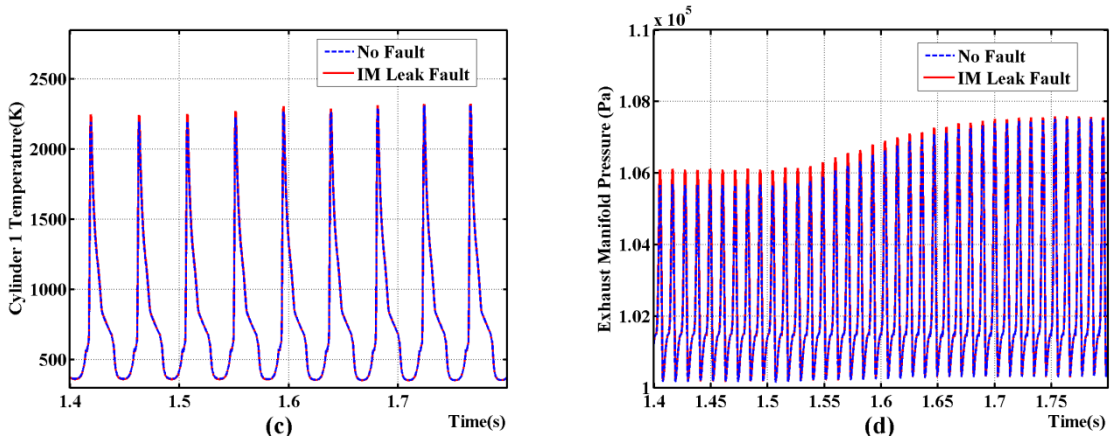

Figure 5: Engine variables under IM leak fault.

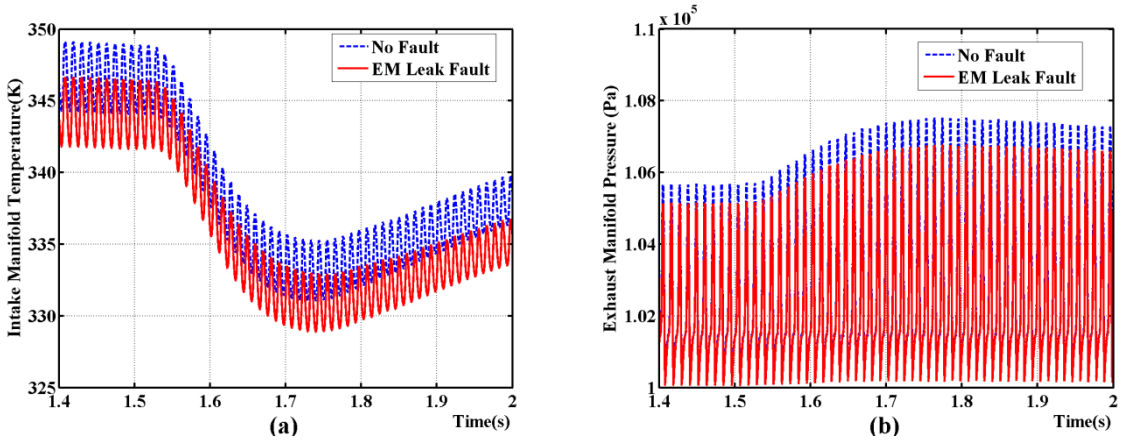

Figure 6: Engine variables under EM leak fault.

Figure **7** shows some of the engine variables under an intake valve leak of 10mm^2 magnitude in one of the cylinders. The affected cylinder pressure drops due to leak. Exhaust manifold variables show deviations from the nominal model every fourth cycle, indicating the fault with one of the four cylinders. The WCCM advantage is well manifested in this case. IM pressure is affected both due to EGR flow and backflow through the leaking valve.

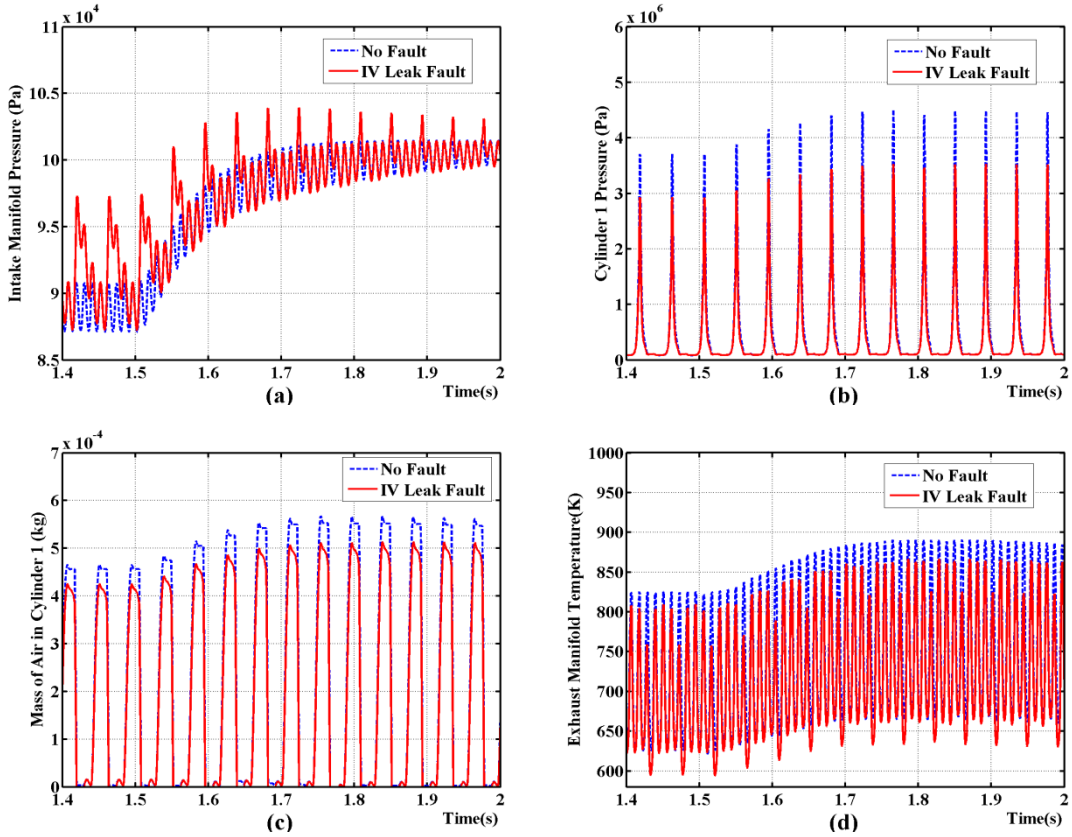

Figure 7: Engine variables under intake valve leak

Figure 8 shows the engine variables for an exhaust valve leak of 10mm^2. It could be seen that while the cylinder variables show similar patterns as the intake valve leak case, the IM and EM variables have different patterns compared with the intake valve leak case. This helps in fault isolation.

Figure 9 shows the engine variables for an injector fault in cylinder 1, simulated by halving the fuel flow to one of the injectors. In the modelling scheme, this fault is incorporated by a multiplicative factor to the fuel flow rate. It could be seen that the effect of such a fault on IM and EM variables is similar to the exhaust valve leak case. But the fuel mass in cylinder – one of the state variables – is identifiably distinct from the valve leak case and could be used for fault isolation.

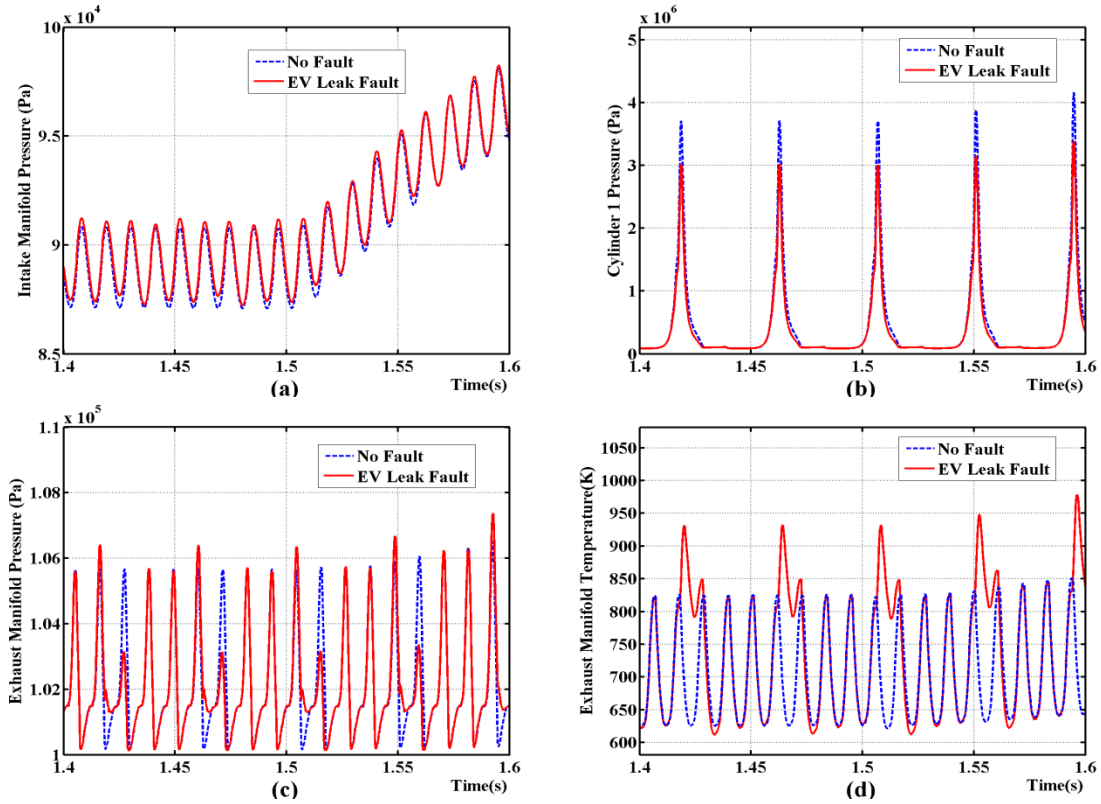

Figure 8: Engine variables under exhaust valve leak

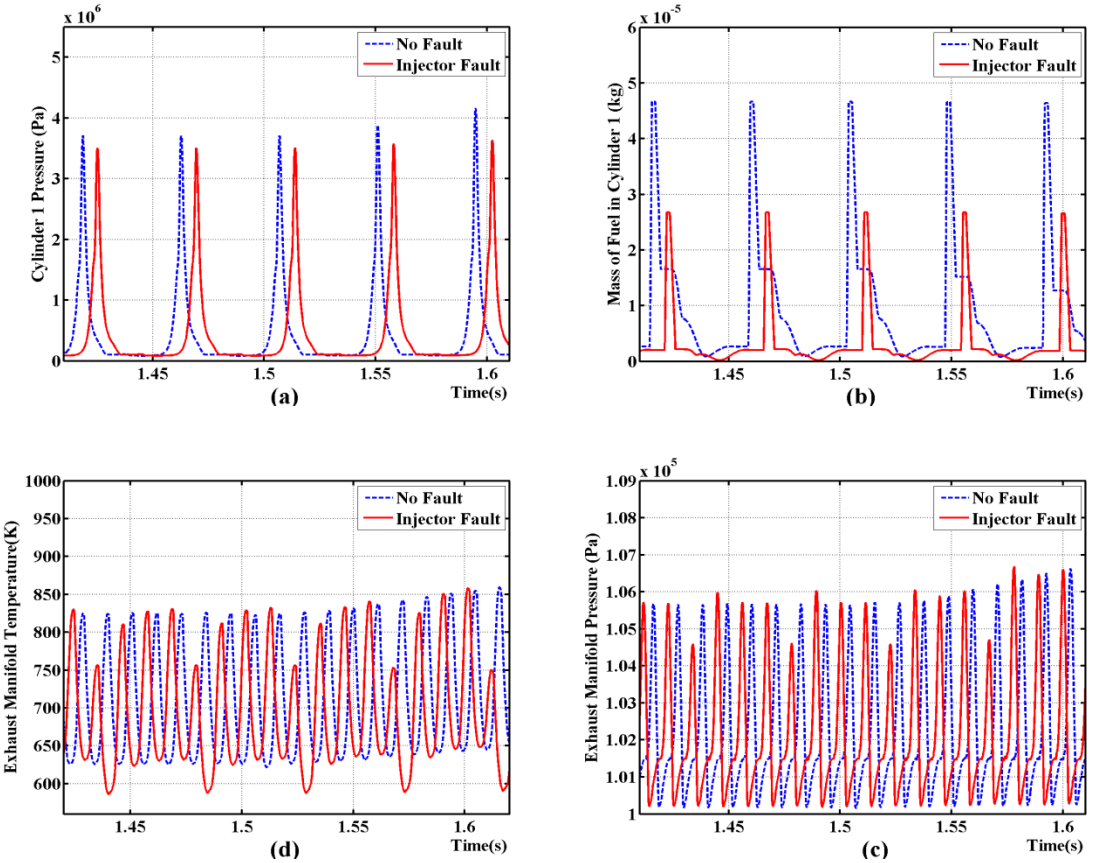

Figure 9: Engine variables under injector fault in cylinder 1

6. Data acquisition from the test engine

In addition to validating the engine model against AMESim simulation, it was also validated against a two cylinder engine with no EGR, that of Tata Nano^{TM}. To this end, all the terms corresponding to EGR have been removed from the state equations. For validation purposes and better fault diagnosability, an additional pressure sensor was fitted at the exhaust manifold of the engine. The sensors associated with the engine system, including the added sensor, are listed in Table 5. The sensor output signals were converted to the variables in appropriate units in the model.

Table 5: Sensors and associated measurements in the engine system

Sl. No	Sensor(s)	Measured variable(s) and range	Sensor output range
1	Throttle Position(TPS)	Throttle position–angle (-5^o to 91^o)	0.05V–0.95V
2	TMAP	Intake manifold temperature (-40^oC to 130^oC) and absolute pressure (10 -115kPa)	50kΩ–100Ω (NTC, approx.) 0.4–4.65V (Pressure)
3	Exhaust pressure Sensor(Kistler)	Exhaust manifold absolute pressure (0-5 MPa)	0-10V
4	Crankshaft position sensor	Crankshaft position and engine speed (20-7000 rpm)	0-200V 36-2 pulses/rev

7. Experimental results

The engine model was experimentally validated against a Tata Nano 2-cylinder engine without EGR. Speed and crank angle signals were extracted using the technique described in 2.1.1. Measurements available from the Nano engine that are of interest to us are: throttle position, IM temperature, IM pressure, EM pressure (added sensor), and crank position. Of these the throttle position serves as an input. The crank position sensor output was used to extract speed and crank-angle signals, again serving as inputs. Model performance for the experimental case had to be compared against the rest of the measurements, as contrasted with the simulation case where they were compared against all the state variables from the AMESim engine model.

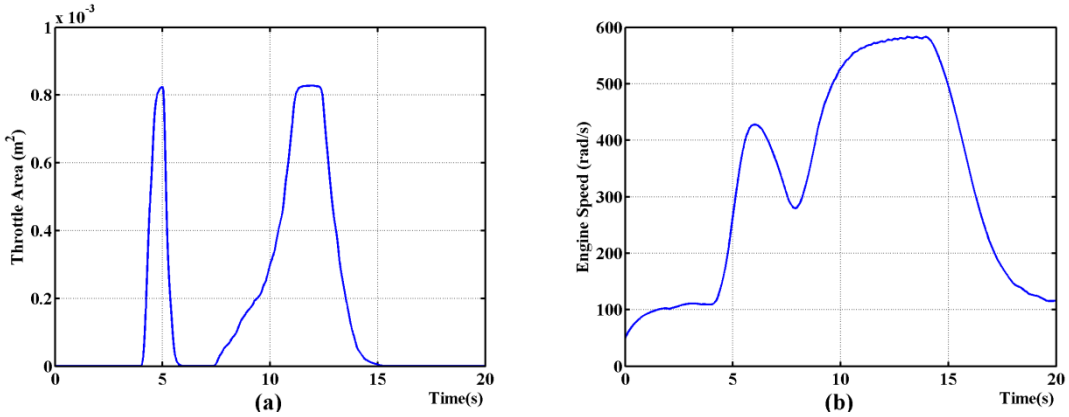

Figure 10: Extracted throttle area and engine speed signals

Figure 10 shows the extracted throttle and speed signals. Note that the speed signal does not capture the within cycle variations because of sampling limitations and filtering. However this was not found to significantly affect the model variables. IM temperature, IM pressure and EM pressure from the engine model, along with actual measurement data from Nano, are shown in Figure 11. Cylinder temperature from the model, shown in the figure for a small time frame for better visibility of within cycle nature, is not a measured variable and can be of use in fault diagnosis. Minor deviations of the model variables from that of actual engine could be corrected using a state estimator for which the measured temperature and pressure from IM and EM respectively could serve as measurement inputs. The IM temperature from the model was filtered to account for the large time constant of the temperature sensor. Note that the measurement noise shows higher variance than the model for all variables, as expected. This suggests the use of estimated signal for fault diagnosis rather than directly using the measurements.

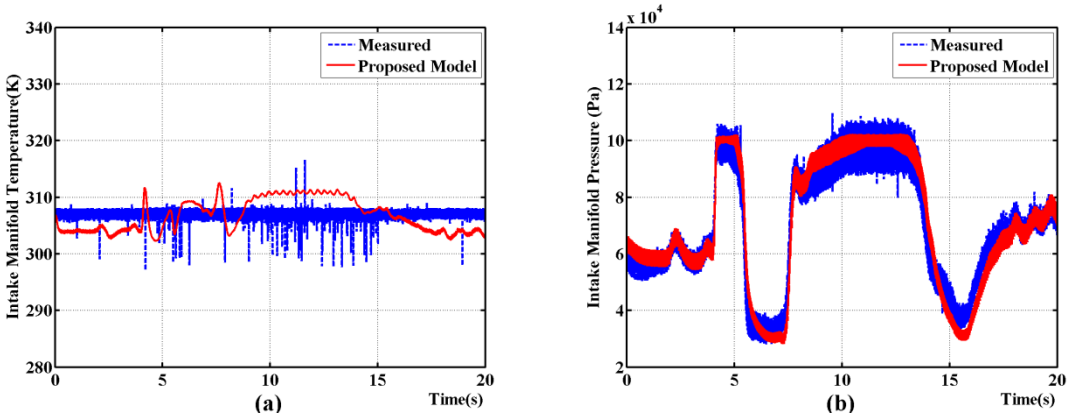

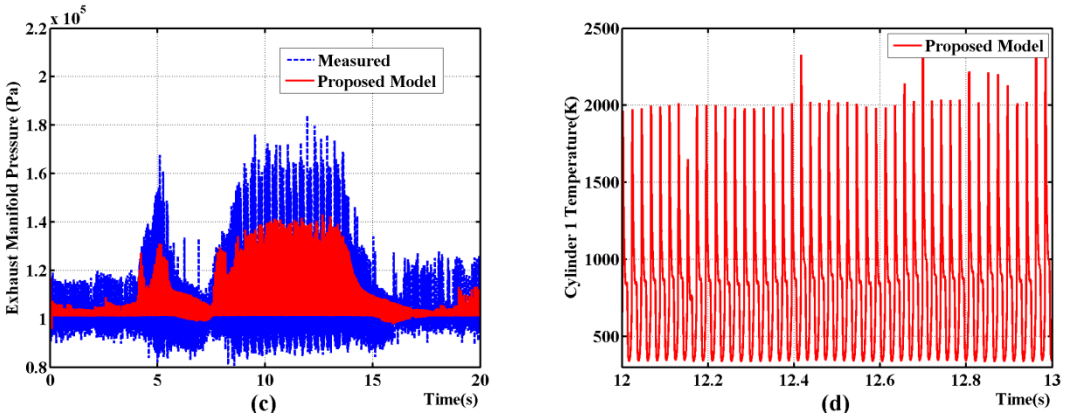

Figure 11: Engine variables from the developed model (Simulink) and real car

8. Conclusion

A non-linear hybrid state space model of s spark-ignition engine was developed towards fault diagnosis. The model was validated by simulation against an AMESim model. Mechanisms for incorporation of faults by suitable parameterization were also demonstrated. Advantages of the model for detection and isolation of various faults were also discussed with the simulation results provided for each case. Finally, the nominal model was validated using data from a real engine. The model could be used in an estimator like Extended Kalman Filter (EKF), to correct for model inaccuracies online using the sensor measurements. Detailed schemes for fault diagnosis are being developed.

Acknowledgement

The support for this work from NPMASS (National Program for Micro and Smart Systems), Govt. of India, is greatly acknowledged. Support for setting up the experimental engine test bed from Tata Motors Engineering Research Centre, Pune, India is also acknowledged.

References

[1] D. Jung and D. N. Assanis, "Multi-zone DI diesel spray combustion model for cycle simulation studies of engine performance and emissions," *SAE transactions*, vol. 110, no. 3, pp. 1510-1532, 2001.

[2] L. Liang and R. D. Reitz, "Spark ignition engine combustion modeling using a level set

method with detailed chemistry," *SAE paper,* no. 2006-01, p. 0243, 2006.

[3] D. J. Torres and M. F. Trujillo, "KIVA-4: An unstructured ALE code for compressible gas flow with sprays," *Journal of Computational Physics,* vol. 219, no. 2, pp. 943-975, 2006.

[4] E. Hendricks and S. C. Sorenson, "Mean value modelling of spark ignition engines," 1990.

[5] M. Fons, M. Muller, A. Chevalier, C. Vigild, E. Hendricks and S. C. Sorenson, "Mean value engine modelling of an SI engine with EGR," 1999.

[6] L. Eriksson, L. Nielsen, J. Brugaard, J. Bergstrom, F. Pettersson and P. Andersson, "Modeling of a turbocharged SI engine," *Annual Reviews in Control,* vol. 26, no. 1, pp. 129-137, 2002.

[7] L. Eriksson, "Modeling and control of turbocharged SI and DI engines," *Oil \& Gas Science and Technology-Revue de l'IFP,* vol. 62, no. 4, pp. 523-538, 2007.

[8] A. Balluchi, L. Benvenuti, M. di Benedetto, C. Pinello and A. Sangiovanni-Vincentelli, "Automotive engine control and hybrid systems: challenges and opportunities," 2000.

[9] A. Balluchi, L. Benvenuti, M. D. Di Benedetto, G. M. Miconi, U. Pozzi, T. Villa, H. Wong-Toi and A. L. Sangiovanni-Vincentelli, "Maximal safe set computation for idle speed control of an automotive engine," in *Hybrid Systems: Computation and Control,* Springer, 2000, pp. 32-44.

[10] M. Nyberg, "Model-based diagnosis of an automotive engine using several types of fault models," *Control Systems Technology, IEEE Transactions on,* vol. 10, no. 5, pp. 679-689, 2002.

[11] M. Nyberg and T. Stutte, "Model based diagnosis of the air path of an automotive diesel engine," *Control Engineering Practice,* vol. 12, no. 5, pp. 513-525, 2004.

[12] M. Rizvi, A. Bhatti and Q. Butt, "Hybrid Model of the Gasoline Engine for Misfire Detection," *IEEE Transactions on Industrial Electronics,* vol. 58, no. 8, pp. 3680-3692,

Aug 2011.

[13] S. Sengupta, S. Mukhopadhyay, A. Deb, K. Pattada and S. De, "Hybrid Automata Modeling of SI Gasoline Engines towards State Estimation for Fault Diagnosis," *SAE International Journal of Engines,* vol. 5, no. 3, pp. 759-781, 2012.

[14] M. A. Franchek, P. J. Buehler and I. Makki, "Intake air path diagnostics for internal combustion engines," *Journal of Dynamic Systems, Measurement, and Control,* vol. 129, no. 1, pp. 32-40, 2007.

[15] A. Schilling, A. Amstutz and L. Guzzella, "Model-based detection and isolation of faults due to ageing in the air and fuel paths of common-rail direct injection diesel engines equipped with a lambda and a nitrogen oxides sensor," *Proceedings of the Institution of Mechanical Engineers, Part D: Journal of Automobile Engineering,* vol. 222, no. 1, pp. 101-117, 2008.

[16] P. Andersson and L. Eriksson, "Detection of exhaust manifold leaks on a turbocharged SI-engine with wastegate," *Electronic Engine Controls 2002. SAE,* 2002.

[17] Y. Shiao and J. J. Moskwa, "Cylinder pressure and combustion heat release estimation for SI engine diagnostics using nonlinear sliding observers," *Control Systems Technology, IEEE Transactions on,* vol. 3, no. 1, pp. 70-78, 1995.

[18] J. Karlsson, J. Fredriksson and others, "Cylinder-by-cylinder engine models vs mean value engine models for use in powertrain control applications," *SAE International, Warrendale, PA, SAE Technical Paper*, pp. 1-906, 1999.

[19] P. Casoli, A. Gambarotta, N. Pompini, U. Caiazzo, E. Lanfranco and A. Palmisano, "Development and validation of a "crank-angle" model of an automotive turbocharged Engine for HiL Applications," *Energy Procedia,* vol. 45, pp. 839-848, 2014.

[20] L. Guzzella and C. H. Onder, Introduction to modeling and control of internal combustion engine systems, Springer, 2010.

[21] J. B. Heywood, Internal Combustion Engine Fundamentals, McGraw-Hill International Editions, 1998.

[22] R. M. Felder and R. W. Rousseau, Elementry principles of chemical processes, John Wiley & Sons, 2008.

[23] W. J. D. Annand, “Heat transfer in the cylinder of reciprocating internal combustion engines,” in *Proceedings of the IMechE, Part D: Journal of Automobile Engineering*, 1963.

[24] J. L. Lumley, Engines: an introduction, Cambridge University Press, 1999.